High frequency band sensitivity of large gravitational wave interferometers

N.I.Kolosnitsin
Earth Physics Institute of RAS, Moscow. Russia

V.N.Rudenko
Sternberg Astronomical Institute, MSU, Moscow.Russia

It is shown that a **reception frequency bandwidth of the large interferometer gravitational wave detectors could be expanded in the high frequency wing up to 100 kHz due to special "windows of reconstructed sensitivity" which have to appear in regions of the EM-gravity resonance**

. We present formula for the value of maximal "reconstructed sensitivity" inside the resonance zones for the case of dominant optical shot noise (other noises are considered as much smaller). Hypothetical high frequency GW sources of astrophysical origin and possible data processing algorithms are also briefly discussed

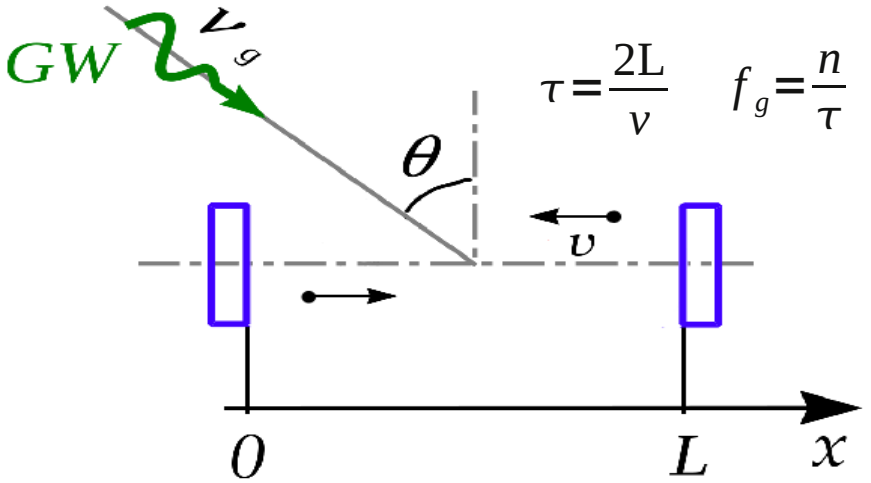

Particle energy accumulation
L.P. Grishchuk Sov.Phys. JETP 66, 833 (1974)

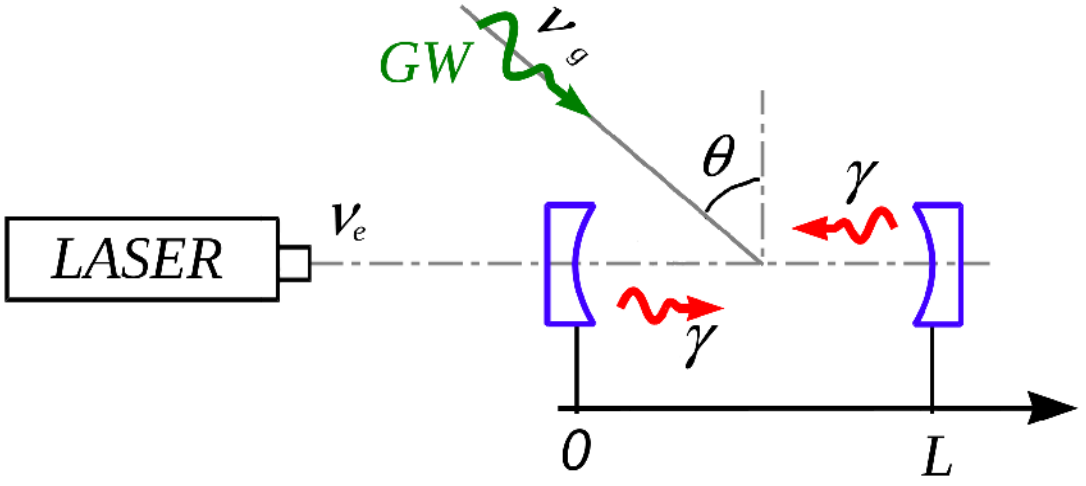

Photon energy accumulation
Rudenko V.N., Sazhin M.V. Sov.Jr. "Quantum Electronics" v.10, n.11, 1366, 1980

Test particles traveling between two flat mirrors. Particles can accumulate energy if the GW frequency ω_g equals an integer number of the circulation frequency $\Omega = \upsilon/2L$, i.e. $\omega_g = n\,\Omega$ (n = 1,2,3…).

$$I = I_0 \cdot \left[1 - 0.5 h_g \frac{\nu_e}{\nu_g} F\left(\cos \omega_g t + \varphi\right)\right]$$

$$Q \sim \frac{L}{\lambda_e} F, \ldots \frac{L}{\lambda_e} \to \frac{\nu_e}{\nu_g}$$

Optical delay line under GW radiation

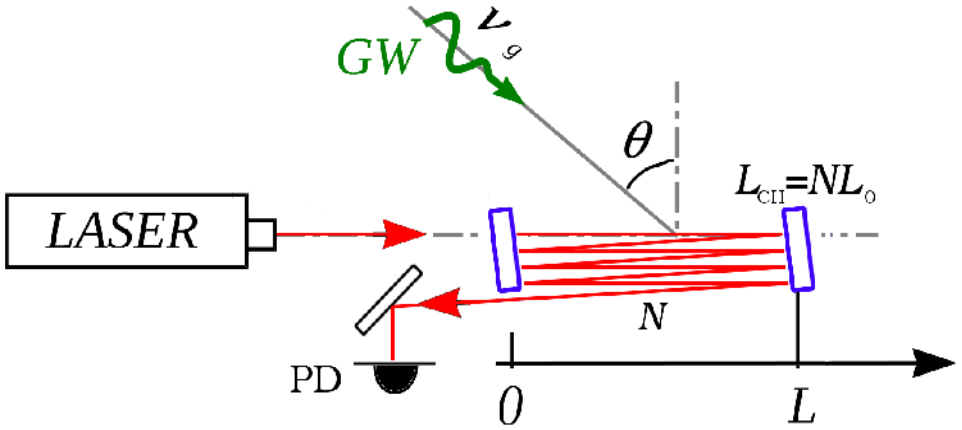

Interferometer configuration

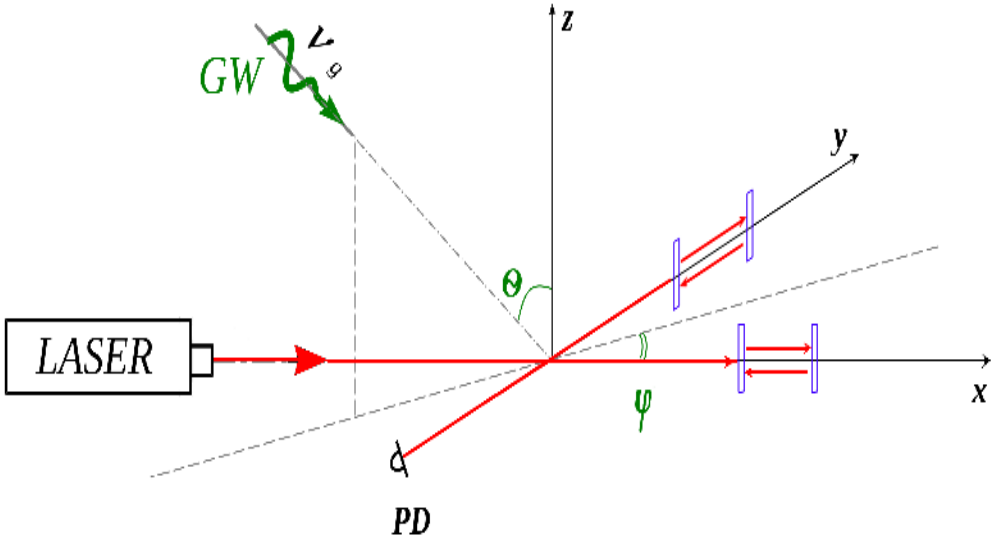

Electrical field of the laser beam going along the x direction through the optical delay line (ODL) in the presence of a gravitational wave (fig.1) can be read as [2]

$$E^{(-)}=\frac{1}{2}r_1^{N-1}r_2^N\exp(i\omega_0 t)\left(h\hat{D}^N A\right)+c.c.$$

$$\boldsymbol{h}=(1,\tfrac{1}{2}h_{11}\exp(i\omega_g t),\tfrac{1}{2}h_{22}\exp(-i\omega_g t)),\qquad A=(E_0,\,0,\,0).$$

-

$\omega_0=2\pi\nu_{em}$

$\omega_g=2\pi\nu_g$ optical and gravitational frequencies;

$$E^{(-)}=-r_1^{N-1}r_2^N E_0 e^{-iN\mu}\frac{1}{2}e^{i\omega_0 t}\left\{1+h_{11}\frac{\mu}{4\varepsilon}\frac{\sin(N\varepsilon/2)}{\sin(\varepsilon/2)}\left[e^{i\omega t}e^{-i(N-1)\varepsilon/2}K_x-e^{-i\omega t}e^{i(N-1)\varepsilon/2}K_x^*\right]\right\}+c.c.$$

$$\mu=2k_0L,\qquad \varepsilon=2k_gL=\omega_g/\nu_0,\qquad \nu_0=c/2L,\qquad \alpha=\sin\theta\cos\varphi$$

Michelson with delay lines in arms

Michelson configuration with delay line arms is presented at (fig.2) Electrical fields of the arm's ODL (6), (7) results in the light intensity at the output photo diode

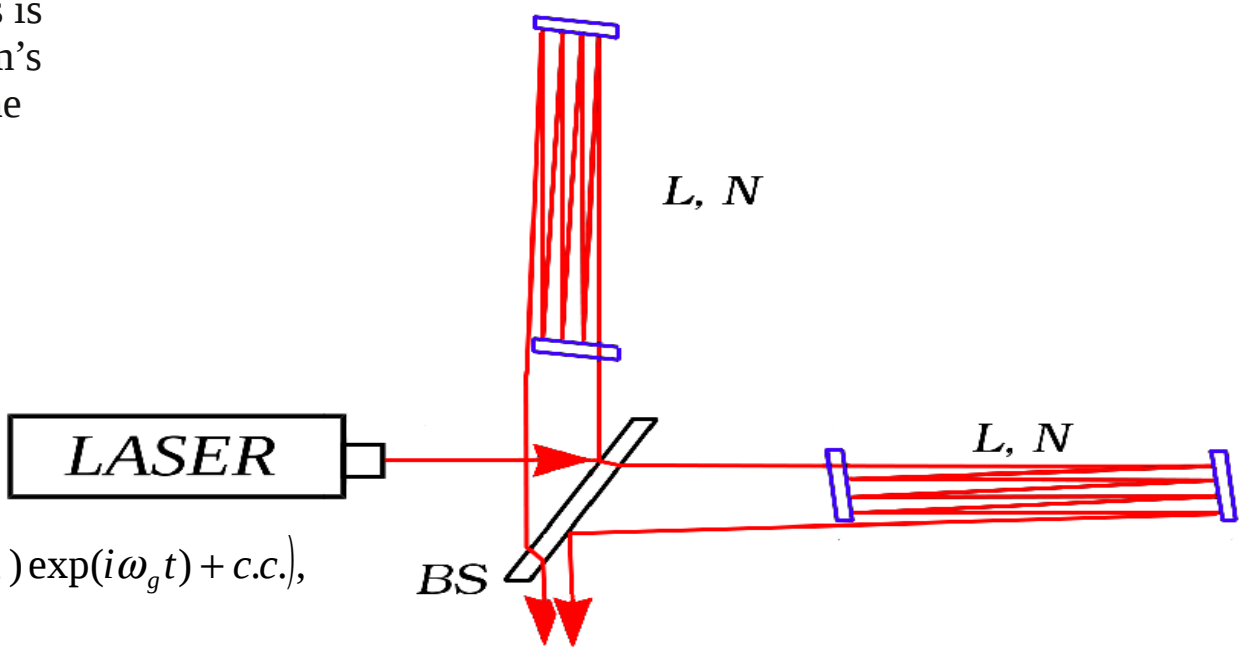

$$I_{\pm} = I_0\left(T_{\pm}(\Delta\mu) + T'_{\pm} h H_{ODL}(i\omega_g)\exp(i\omega_g t) + c.c.\right),$$

where

$$T_{\pm}(\Delta\mu) = 1 \pm \cos(N\Delta\mu), \qquad T'_{\pm} \equiv \frac{dT_{\pm}}{d(\Delta\mu)} = \mp\sin(N\Delta\mu),$$

and $H(\omega_g)$ is a transfer function of the interferometer as a GW detector.

$$H\ (\omega_g) = -i\frac{\mu}{4\varepsilon}\frac{\sin(N\varepsilon/2)}{\sin(\varepsilon/2)}\exp(-i(N-1)\varepsilon/2)\cdot F(\varepsilon,\vartheta,\varphi)$$

The factor $F(\varepsilon,\theta,\varphi)$ is the detector antenna pattern. In a general case this pattern will be frequency dependent (!)

$$F(\varepsilon,\theta,\varphi) = K_x(\varepsilon,\alpha)\frac{h_{11}}{h} - K_y(\varepsilon,\beta)\frac{h_{22}}{h},$$

a) ***long wave approximation*** : $\lambda_g >> L$; in this situation $\varepsilon << 1$

$H(\omega_g)$ is factorized separating a frequency transfer function and angular antenna pattern.

$$H_{LW} = \frac{\mu}{4}\frac{\sin(N\varepsilon/2)}{\sin(\varepsilon/2)} F_0(\theta,\varphi), \quad \varepsilon=(\omega_g/\nu_0) << 1. \qquad (**)$$

$F_0(\theta,\varphi)$ is the angular antenna pattern

$$F_0(\theta,\varphi) = (h_{11} - h_{22})/h = (h_+/h)(1+\cos^2\theta)\cos 2\varphi - (h_\times/h)2\cos\theta \sin 2\varphi.$$

b) opto – gravity resonance

In resonance $\nu_g^{(n)} = n\nu_0$, with $\varepsilon/2 = \pi(\nu_g^{(n)}/\nu_0) = \pi n$. Under the integer number of n (n = 1, 2, 3…) the ratio $\sin(N\varepsilon/2)/\sin(\varepsilon/2)$ has an uncertainty type of 0/0.
Taking a small frequency deviation ν_g from $\nu_g^{(n)}$ one introduces an undimentional detuning

$$x = \frac{\nu_g - n\nu_0}{\nu_0} = \frac{\Delta\nu_g}{\nu_0} \; ; \qquad \nu_g/\nu_0 = n + x, \text{ и } \varepsilon/2 = \pi(\nu_g/\nu_0) = \pi(n+x)..$$

It results in

$$H_{GOR}(n,x,\theta,\varphi) = -i\frac{\mu}{8\pi}\frac{1}{n}\frac{\sin(\pi N x)}{\sin(\pi x)} F(n,\theta,\varphi), \qquad (***)$$

here the antenna pattern $F(n,\theta,\varphi)$ depends on frequency $\nu_g{}^{(n)} = n\nu_0$

[Both formulae (**) and (***) contents the “Buys-Ballot” factor $\sin Nx / \sin x$, so that

$$\frac{\sin(N\varepsilon/2)}{\sin(\varepsilon/2)} = \frac{\cos\pi Nn}{\cos\pi n}\frac{\sin\pi Nx}{\sin\pi x}\Big|_{x\to 0} = (-1)^{(N-1)n}\lim_{x\to 0}\frac{\sin\pi Nx}{\sin\pi x} = (-1)^{(N-1)n} N.$$

this factor filters harmonics n π]

Width of resonance

For a comparison the Buys-Ballot factors in the “long wave” limit (zero resonance $n=0$) (**) and OG resonance (***) are presented at (fig.3) (ν_0 = 37,572 kHz for LIGO interferometers, N = 200)

$$f_1(x) = \frac{\sin(\pi N x)}{\pi x} \left(= \frac{\sin N\varepsilon/2}{\varepsilon/2} \right),$$

$$f_2(x) = \frac{\sin(\pi N x)}{\sin(\pi x)} \left(= \frac{\sin N\varepsilon/2}{\sin(\varepsilon/2)} \right),$$

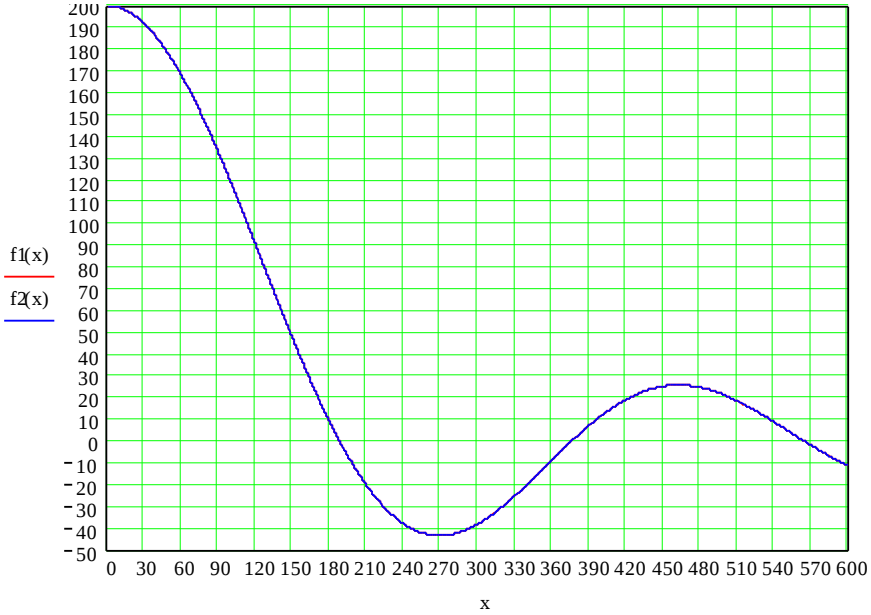

(detuning x is taken in Hz, both curves (“blue” and “red” coincides)

the bandwidth at the level 0,5 is estimated as ~ 113 Hz , (x = 0.00327).

Michelson transfer function with EM- gravity resonances

At (fig.4) the total transfer function of Michelson GW- detector is presented taking into account the existence of FM-gravity resonances (following parameters were selected for calculation:
ν_0 = 37,572 kHz , N = 200, $F(n,\theta,\varphi)$ was replaced by its maximum)

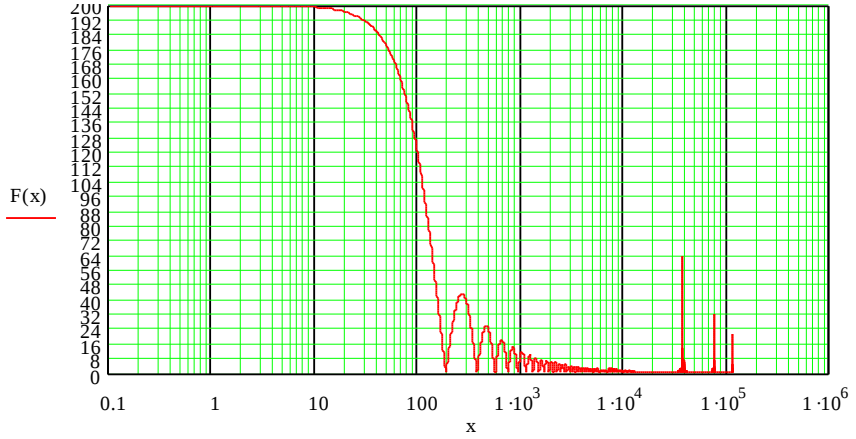

at the picture (fig.4) the low frequency zone and first three opto –gravity resonances are shown.
For to show the high frequency part the fig.4 was recalculated with *N = 20*

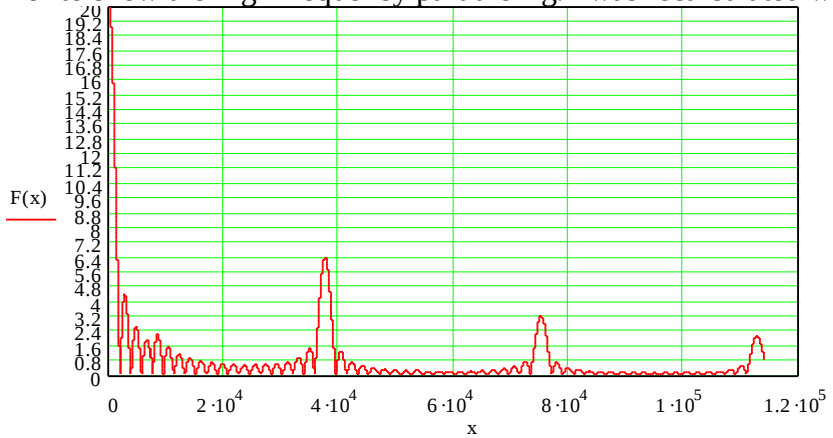

the first three EM-gravity resonance zones for LIGO, supposing *N = F*, correspond to frequencies: 37,572 kHz, 75,144 kHz, 112,716 kHz.. Width of zone is on the order of the “low frequency window” ~ 100 Hz.. Its amplitude decrease as ~ $1/\omega_g$

Total high frequency sensitivity curve of large interferometers

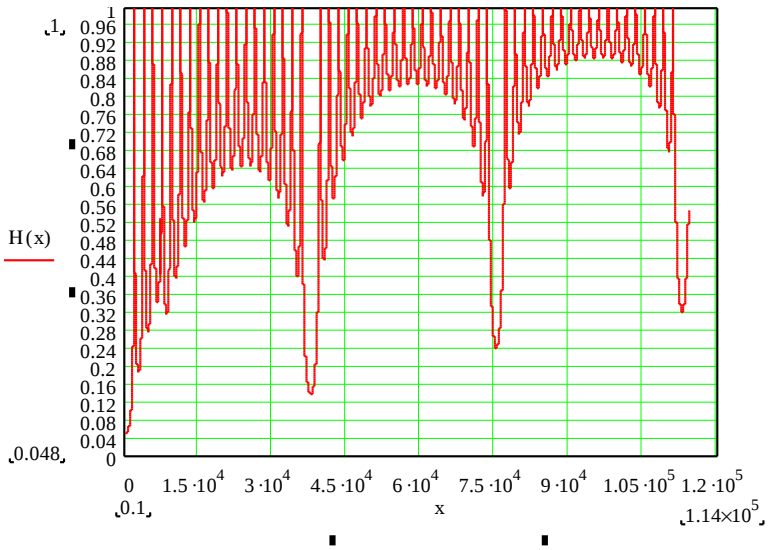

At the white photon noise background the detection sensitivity is inverse proportional to the transfer function of the interferometer (fig.4). It is given at the fig.5 for ideal mirrors without loses. Absorption smooths the mathematical effect of parasitic oscillation and leads to the plain curve presented at the fig.6

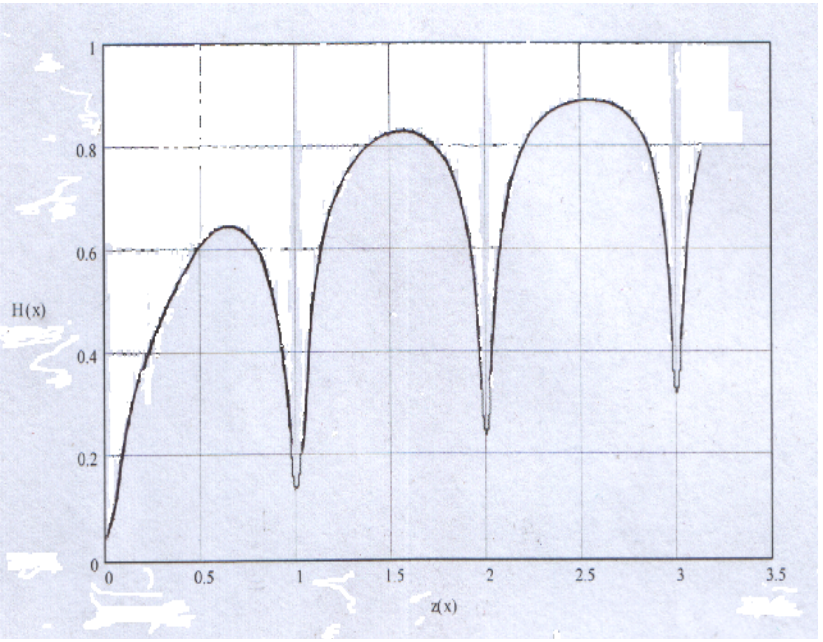

for LIGO 37,5 kHz, 75,1 kHz 112,7 kHz.

Maximum “reconstructed sensitivity” inside the resonance zones for the case of optical shot noise according to the simple “detection rule” $\Delta P_s \geq \Delta P_{fl}$ is estimated as

$$P_0 H_{GOR} h \geq (2\hbar\omega P_0 \Delta f)^{1/2} \quad \text{or} \quad h_{\min} \geq \frac{\lambda \cdot n}{L N} \sqrt{\frac{\hbar\omega \cdot \Delta f}{P_0}}$$

Substitution of the parameters:
P = 30 W, L = 4 km, results in **h ~ 5.10^{-22}n** Hz^{-1/2}

Astrophysics

Conceivable sources for frequency region (10 – 100) kHz could be quark stars and primordial mini black holes [4,5,6]

References

1. Rudenko V.N., Sazhin M.V. Sov. Jr. “Quantum Electronics” v.10, n.11, 1366, 1980
2. Vinet J-Y. Recycling interferometric antennas for periodic gravitational waves. J.Physique. Vol. 47 (1986), 639-643.
3. Kolosnitsyn N.I. The Maxwell equations and gravitational wave detection. Gravitation & Cosmology. 1996, Vol. 2, No 3(7), pp. 262-266.
4. Haensel P., Potekhin A.Y., Yakovlev D.G. Neutron Stars. Springer-Verlag, 2007
5. Haensel P. et.al. A&A, v.50, p.605 , 2009
6. Bisnovatyi-Kogan G.S., Rudenko V.N. Class.Quantum Grav., v.21, p3347, 2004

Antenna pattern configuration

Specific feature of the antenna pattern: – an angular position of the maximum sensitivity depends on the number of resonance (or its frequency); besides its directivity (sharpness) enhances with a growing the resonance number.
Thus an angular position of a source will be defined more accurate compare with the angular precision in the low frequency limit. Structure of the pattern in the cross section $\varphi = \pi/4$, including the case of "zero resonance" are given at fig. 7

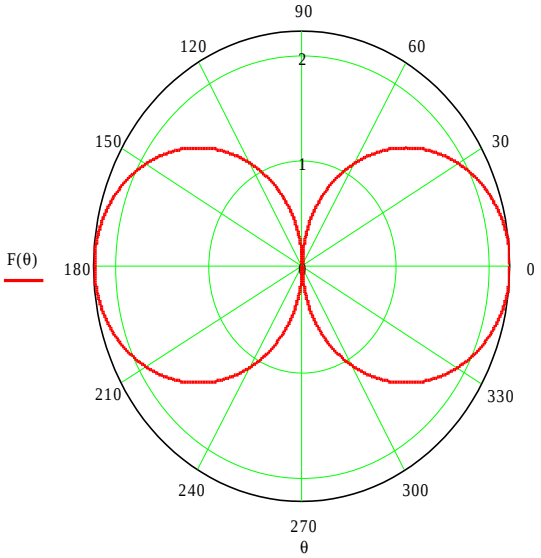

n = 0 , max F = 2.221

n = 2 , max (1/2)F = 1.385

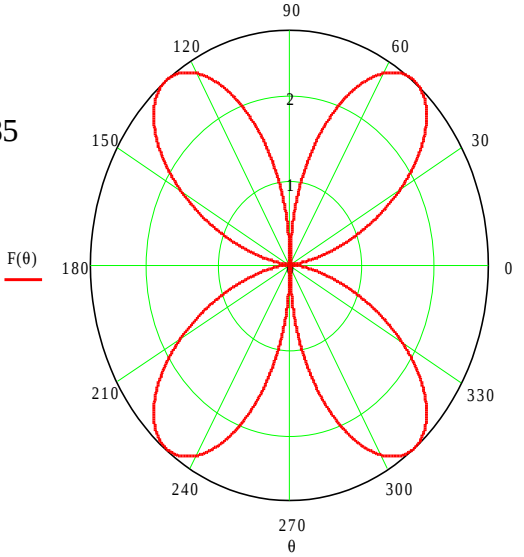

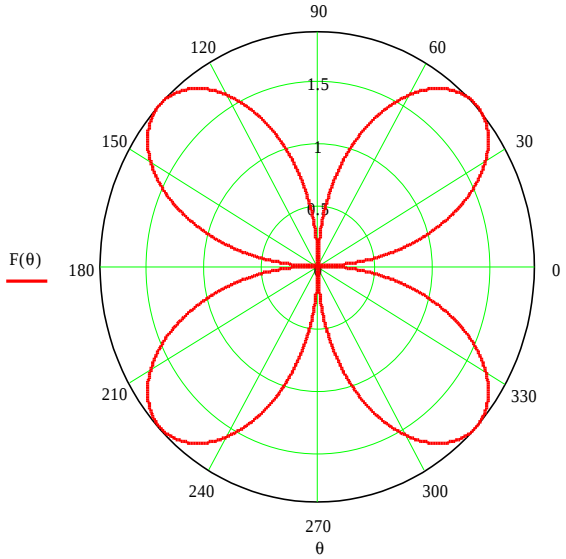

n = 1 , max F = 1.889

n = 3 , max (1/3)F =0.98